International Journal of Applied Engineering Research ISSN 0973-4562 Volume 10, Number 21 (2015) pp 41730-41737

Experimental Performance of Flat-Plate Thermosyphon Solar Water Heaters with Copper Oxide Nanofluids

D. Anin Vincely[a,*], E. Natarajan[b]

Institute for Energy Studies, Anna University, Chennai 600 025, Tamil Nadu, India
[*] Corresponding author. Tel.: +91 94451 15278, E-mail: vincely_zeal@yahoo.com
[a] Research scholar. [b] Professor. E-mail: enat123@gmail.com

Abstract
Experiments were conducted on a thermosyphon-type flat-plate collector for water heating application. The thermosyphon has five parallel, black-coated copper tubes positioned between the inlet and outlet headers. The assembly was placed inside an insulated chamber with a glass cover at the top and inclined at 45°. Water and water-based nanofluids were used as the working medium to absorb heat from solar rays. Copper oxide nanoparticles of 40-50 nm in size were added to the base fluid at 0.1, 0.2, 0.3 and 0.5 wt.%. Hot working fluid was made to flow in the shell side of a heat exchanger, where the utility water was sent through a helically coiled copper tube. Temperatures of collector at strategic locations, temperatures of inlet and outlet working fluid, and temperature of the utility water were measured. The experimental results revealed that utilizing nanofluid increases the collector efficiency in comparison with water as an absorbing medium. An enhancement in collector efficiency of about 5.65% was obtained for a mass flow rate of 0.0033 kg/s for 0.2 wt.% of copper oxide nanofluid. It was found that by increasing weight fraction of the nanoparticles, the efficiency of the collector was improved.

Keywords: Thermosyphon solar heaters, Nanofluids, Collector efficiency, Helical coil tube.

1. Introduction

Solar thermal technology converts the energy of sun directly into heat, which is stored in the form of a heated fluid, using water as a working fluid. The typical solar heating system consists of a collector-a heat transfer circuit that includes the fluid and the means to circulate it-and a storage system including a heat exchanger. Based on the principle of thermosyphon, the hot water is passed through the collector and rises by natural convection in the hot water storage tank. Simultaneously, due to gravity the cold water in the cold water tank descends to the bottom header of the collector. Therefore, the circulation of water in the hot water storage tank occurs due to the increase in temperature and volume. The circulation persists as the process is repeated. Compared with forced circulation, the thermosyphon system has a high impact in domestic sector due to its ease of operation, simplicity and less maintenance and non-dependence on hydraulic pump.

Zerrouki *et al.* (2002) considered the natural circulation of a compact thermosyphon solar water heating system that was produced and commercialized in Algeria. The mass flow rate and rise in temperature of the fluid and absorber inside the thermosyphon of a parallel tube design were measured.

Nada *et al.* (2004) designed a two-phase closed thermosyphon solar collector with a shell and tube heat exchanger. The influence of the cooling water mass flow rates, the inlet cooling water temperature and the number of the thermosyphon tubes on the thermal performance of the collector was experimentally studied.

The low thermal conductivity of conventionally used, low-cost and abundantly available heat transfer fluid such as water is considered as a primary limitation in the thermal systems. A fluid with enhanced thermophysical properties could lead to improvements in the performance of a thermosyphon. Nanofluids are extensively used by several researchers for various applications, who claim enhanced performance or increased heat transfer rates in their thermal systems.

The term ‘nanofluid’ was first coined by Choi (1995). As the nanofluid greatly enhances the heat transfer properties in the base fluids, it is ideal for several practical applications. An increased thermal conductivity, liquid viscosity and heat transfer coefficient are unique properties of nanofluids. The thermal conductivity of metallic nanofluids is found to be greater than that of non-metallic liquids.

In comparison with the suspensions of millimeter/micrometer-sized particles, nanofluids show better stability, enhanced rheological properties and considerably higher thermal conductivity. The thermophysical properties of nanofluids along with the chaotic movements of ultrafine particles in the fluid, which accelerate energy exchange, are suggested to be the key factors for the observed heat transfer. Hence, nanofluids are promising working medium in coolants, lubricants, hydraulic fluids and metal cutting plates.

Lee *et al.* (1999) suggested ultrasonic vibration of nanofluids and addition of surfactants help in enhancing the suspension of nanoparticles in the base fluid for longer periods without agglomeration. Thermal conductivity is an important parameter for assessing the heat transfer enhancement of nanofluids. Wang *et al.* (1999) measured thermal conductivity in nanofluids containing aluminium oxide (Al_2O_3) and copper oxide (CuO) nanoparticles and investigated the effect of base fluids on the thermal conductivity of nanofluids. Otanicar *et al*. (2010) investigated both experimentally and numerically the effects of different nanofluids such as carbon nanotubes, graphite and silver on the performance of a micro-scale direct absorption solar collector. He analysed experimentally the effects of different nanofluids on the efficiency of the micro-solar thermal collector. He reported an improvement in

efficiency of up to 5% in solar thermal collectors using nanofluids as the absorption medium.

Lu *et al.* (2011) have studied experimentally the effect of CuO-water nanofluid on the efficiency of the high-temperature-evacuated tube solar collectors. They showed that utilizing the nanofluids as the absorption medium can significantly enhance the thermal performance of the evaporator and evaporating heat transfer coefficients may increase by about 30% compared with those of water.

Yousefi *et al*. (2012a) investigated experimentally the effects of Al_2O_3-water nanofluid on the efficiency of flat-plate collector. They showed that using Triton X-100 as surfactant to base fluid, there was an enhancement in heat transfer. They showed that efficiency of the solar collector with 0.2 wt. fraction of nanofluid is higher than that of water by 28.3%.

Yousefi *et al.* (2012b) investigated experimentally the effects of multi-walled carbon nanotube (MWCNT)-water nanofluid on the efficiency of flat-plate collector. The results showed that by increasing the weight fraction from 0.2% to 0.4%, there was a substantial increase in efficiency. Yousefi *et al.* (2012c) also investigated the effect pH variation in MWCNT-water nanofluid on the efficiency of flat-plate collector and observed greater difference between the pH of nanofluid and the pH of isoelectric point leads to higher efficiency.

Wei *et al*. (2013) developed a mathematical model for the heat transfer process inside the new collector and reasonable empirical correlations of heat transfer coefficients are adopted to calculate the work efficiency. The collector efficiency shows the same tendency with the solar radiation. In addition, the collector efficiency could get further improved by keeping vacuum state inside the solar heat collector. Shojaeizadeh *et al*. (2014) studied the effect of propylene glycol/water at various concentrations ranging from 0 to 100 wt.% of glycol on the efficiency of a flat-plate solar collector. Increasing propylene glycol volume concentration from 25% to 75% enhances the efficiency of the flat-plate solar collector.

Goudarzi *et al*. (2014) investigated experimentally the collector performance for a cylindrical solar collector with receiver helical pipe. The results showed that for 0.1 wt.% CuO nanofluid in 0.0083 kg/s mass flow rate, the maximum thermal efficiency of this collector is increased in comparison with water by 25.6%.

Ali Jabari *et al.* (2014) have carried out experimental studies on the effect of CuO-water nanofluid on the efficiency of flat-plate collector and investigated that for any particular working fluid, there is an optimum mass flow rate that maximizes the collector efficiency. Chougule *et al*. (2014) studied the effect of the tilt angle of the solar collector at various concentrations of nanofluids to find the optimal concentration for the maximum performance and observed that the efficiency of the heat pipe collectors for both water and nanofluids increases with the tilt angle and decreases when the tilt angle exceeds 50°. It is necessary to apply solar energy to a wide range of applications and provide solutions by modifying energy proportion, improving energy stability, increasing energy sustainability and enhancing system efficiency. The discussion above presents a review of the former studies conducted by various researchers on the application of nanofluids in solar thermal engineering systems.

Nanofluid application in a thermosyphon is relatively new and in particular with buoyancy driven flows, no work has been found reported. Hence, the objective of this study is to investigate different concentrations of a CuO-based nanofluid as a volumetric absorber on the thermal performance enhancement of a flat-plate thermosyphon, without any external pump.

2. Experimental Details

2.1 Preparation of nanofluids

Copper oxide nanoparticles of 40 nm in size were used to prepare nanofluids. The nanoparticles were initially mixed with the base fluid in a magnetic stirrer. In order to enhance the dispersion behaviour, nanoparticles were dispersed by ultrasonic vibration using ultrasonic sonicator and using surfactants such as sodium dodecyl sulphate and sodium dodecyl benzene sulfonate. The sonication time was selected to be 60 min. Sodium dodecyl benzene sulfonate used as the non-ionic surfactant is an ideal dispersing agent for making CuO nanofluids. The nanofluid is stable for 10-15 days and tests are conducted during this period. Nanofluids with different particle volume concentration were prepared to investigate the effect of the nanoparticle concentrations on the performance of solar water heaters.

Scanning electron microscope (SEM) imaging for CuO nanoparticle suspension was made by placing few drops of the dispersion on a copper grid and evaporating them prior to observation. Figure 1 shows the SEM images of CuO nanoparticle at different levels of magnification which indicates that the morphology of particle is spherical in shape and shows very tiny agglomerates. Figure 2 shows the high-resolution transmission electron microscopy (HR-TEM) images of CuO nanofluid at different levels of magnification.

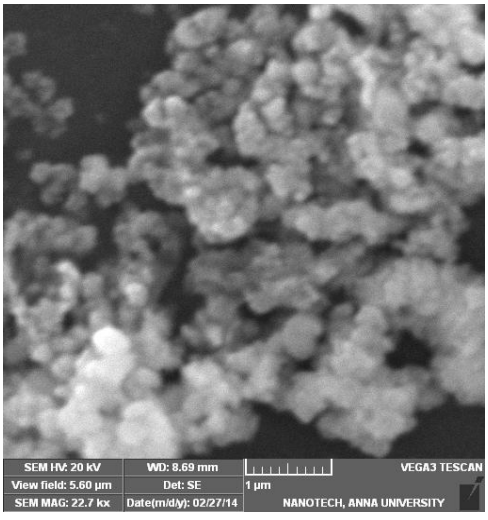

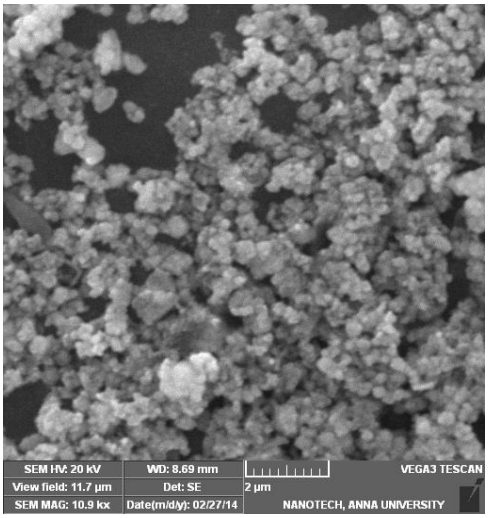

Figure 1. SEM images of CuO nanoparticle suspension with concentration of 0.2 wt.%.

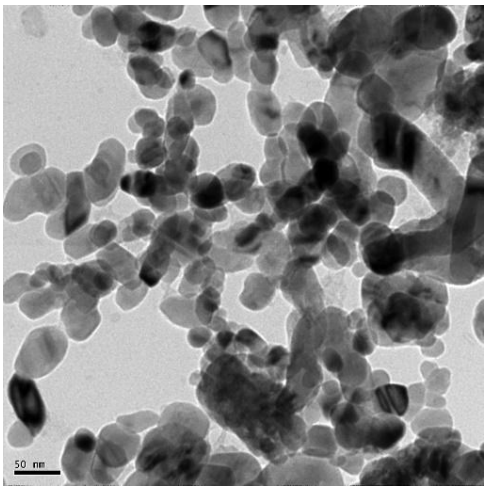

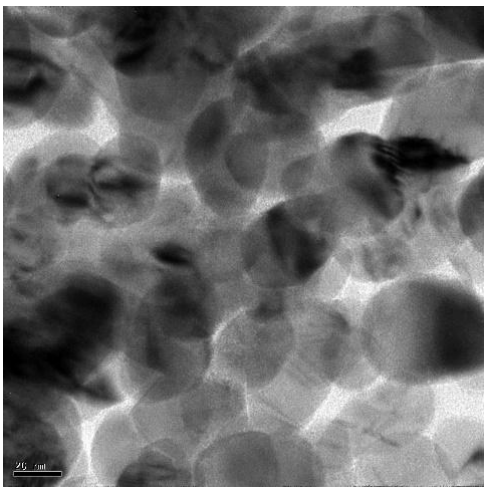

Figure 2. HR-TEM images of CuO nanoparticle suspension with concentration of 0.2 wt.%.

2.2 Experimental set-up and test procedure

Figures 3 and 4 show the schematic sketch and the image of the experimental set-up, respectively. The test set-up consists of (1) a thermosyphon-type flat-plate solar collector, through which the nanofluid circulates and (2) a shell and coil type heat exchanger, through which the service water will be circulated. A storage tank of 30 L capacity was used for the service water circulation, where the fluid temperature increases continuously. Nanofluid exiting the heat exchanger flows into the collector by gravity in the negative *z* direction and rises up inside the thermosyphon by buoyancy. The absorption surface area of the flat-plate collector is 720 mm × 20 mm (i.e., 0.3 m^2). J-type thermocouples were used for measuring the temperatures at strategic locations in the test set-up and a flow meter to measure the working fluid mass flow rate. The thermocouples were shown as encircled numbers and the identification of the thermocouple is given in Figure 3.

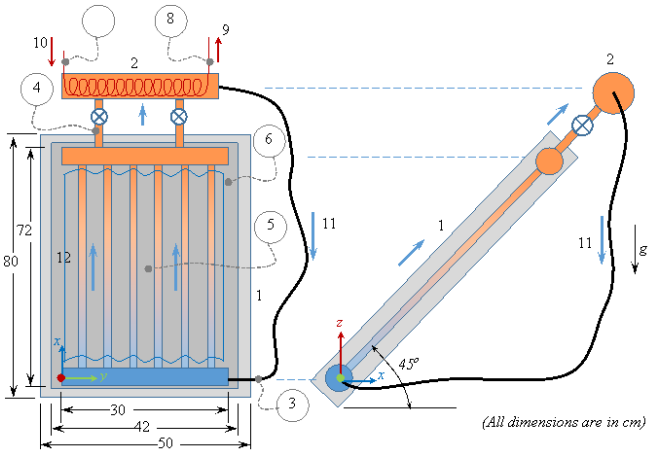

(a) Plan view (b) Side view

1. Flat-plate thermosyphon collector. 2. Heat exchanger. 3. Collector inlet temperature. 4. Collector outlet temperature. 5. Absorber plate temperature. 6. Glass plate temperature. 7. Heat exchanger inlet temperature. 8. Heat exchanger outlet temperature. 9. Service water storage tank. 10. Service water loop. 11. Nanofluid loop. 12. Corrugated aluminium sheet.

Figure 3. Schematic sketch of the experimental set-up.

Figure 4. Image of the thermosyphon solar water heater experimental set-up.

The detailed specifications of the flat-plate collector are provided in Table 1.

Table 1. Specifications of the thermosyphon-type flat-plate collector.

Specification	Dimension	Unit
Occupied area	0.8 × 0.5	m^2
Absorption area (A_c)	0.72 × 0.42	m^2
Collector glazing (glass)	0.003	m
Diameter of upper and lower headers (OD)	0.025	m
Length of the upper and lower headers	0.3	m
Length and diameter of the riser (OD)	0.6,0.012	m
No. of riser tubes	5	-
Specific heat of water (C_p)	4180	J/kgK
Density of CuO nanofluid (ρ_{nf})	6300	kg/m^3
Collector inclination angle w.r.t. the horizontal	45	°

Note. OD = outer diameter.

The heat exchanger is shell and coil type made of copper and is insulated. The dimensions of the shell are 55 mm in diameter and 400 mm long. The helical coil inside the shell was made from a copper tube of 6 mm in diameter and a length of 4500 mm. The thickness of the fin is 0.5 mm, thickness of copper coil is 1 mm and the tilt angle of the solar collector is fixed at 45°. The flow rates are controlled by means of valves. The water and nanofluid flow meters are calibrated by measuring the collected water over a certain period of time. A corrugated aluminium sheet was used to cover the thermosyphon tubes, which are made to have a good contact with the sheet. This sheet was provided to increase the heat transfer surface area exposed to the solar insolation. The surfaces exposed to the solar radiation were coated black to increase the absorption of solar energy.

3. Efficiency Calculations

ASHRAE standards suggest performing the tests in various inlet temperatures. The useful energy gain from the collector is calculated from the following Eq. (1). The useful energy can also be expressed in terms of the energy absorbed and lost from the absorber as given by Eq. (2).

$$Q_u = \dot{m}C_p(T_o - T_i) \quad (1)$$

$$Q_u = A_c F_R\left[G_T(\tau\alpha) - U_L(T_i - T_a)\right] \quad (2)$$

The instantaneous collector efficiency relates the useful energy to the total radiation incident on the collector surface by Eqs. (3) and (4).

$$\eta_i = \frac{Q_u}{A_c.G_T} = \frac{\dot{m}C_p(T_o - T_i)}{G_T} \quad (3)$$

$$\eta_i = F_R(\tau\alpha) - F_R U_L\left(\frac{T_i - T_a}{G_T}\right). \quad (4)$$

The heat removal factor F_R is calculated by

$$F_R = \frac{\dot{m}C_p(T_o - T_i)}{A_c\left[G_T.(\tau\alpha) - U_L(T_o - T_a)\right]}. \quad (5)$$

The experimental mass flow rate is obtained by establishing a balance in heat and mass transfer between the inlet and the outlet collector hot fluid, according to the relation:

$$G_T(\tau\alpha)\eta_i A_c = \dot{m}_{ex}C_p(T_o - T_i) \quad (6)$$

with the instantaneous (η_i) efficiency expressed as

$$\eta_i = \frac{Q_u}{A_c.G_T} = F'(\tau\alpha) - F'U_L\left(\frac{T_{mc} - T_a}{G_T}\right). \quad (7)$$

Substituting η_i, by its expression in Eq. (7), into Eq.(6), we obtain

$$\dot{m}_{ex} = \frac{G_T(\tau\alpha)A_c}{C_p(T_o - T_i)}\left[F'(\tau\alpha) - F'U_L\left(\frac{T_{mc} - T_a}{G_T}\right)\right] \quad (8)$$

with

$$T_{mc} = \frac{T_{tp} + T_i}{2}. \quad (9)$$

The collector efficiency factor for the corrugated absorber plate located between the tube and glass cover is calculated by

$$F' = \frac{1}{1 + U_L\left(\frac{h_1}{\sin\phi/2} + \frac{1}{(h_2)^{-1} + (h_r)^{-1}}\right)^{-1}} \quad (10)$$

where h_1, h_2 and h_r are the convective, wind and radiative heat transfer coefficient between absorber and the glass cover. U_L is the heat loss coefficient for the collector.

The specific heat capacity of a nanofluid can be calculated using the Pak and Cho (1998) correlation as follows:

$$(\rho C_p)_{nf} = \varphi(\rho C_p)_{np} + (1-\varphi)(\rho C_p)_{bf}, \quad (11)$$

where φ indicates the volume fraction of nanoparticles, $C_{p,nf}$ the heat capacity of nanofluid, $C_{p,np}$ the heat capacity of nanoparticles and $C_{p,bf}$ the heat capacity of base fluid (water), which are equal to 551 and 4180 J/kgK, respectively.

$$\rho_{nf} = (1-\varphi)\rho_{bf} + \varphi\rho_{np} \quad (12)$$

The properties of the CuO nanofluid as obtained by the Eqs. (11) and (12) are given in Table 2. The thermal conductivity of nanofluids was measured with the aid of a KD2-pro thermal property meter which works on the basis of transient hot wire method. Three different set of readings are taken for a particular volume fraction and optimization of data is done and thermal conductivity is measured within 30 min from the preparation of nanofluid.

Table 2. Properties of CuO nanofluid.

Volume concentration φ (%)	Density (kg/m^3)	Heat capacity (J/kgK)	Thermal conductivity (W/mK)
0.015	1079.5	4123	0.635
0.032	1169.6	4065	0.680
0.047	1249.1	4008	0.691
0.079	1418.7	3892	0.725

3.1 Uncertainty analysis

Uncertainty analysis is needed to prove the accuracy of the experiments. In this study, uncertainty analysis focuses on the measured and calculated parameters. The calculation of the combined uncertainty of several independent parameters is based on the root-sum-square model presented by Abernethy *et al.* (1983). The wind speed was implemented by a PROVA (AVM-07) anemometer type with ±2% accuracy. The error for TM-207 solar power meter was about ±2%. The error for the J-type thermocouple for temperature measurement is ± 0.1°C.

3.2 Uncertainties on calculated parameters

According to Eq. (4), the experimental uncertainties of the collector efficiency, based on Norton's uncertainty analysis (2010), can be calculated as:

$$U_{\eta_{i(x)}} = \eta_i \times \sqrt{\left(\frac{U_{F_R}}{F_R}\right)^2 + \left(\frac{U_{U_L}}{U_L}\right)^2 + \left(\frac{U_{\Delta T_{ia}}}{\Delta T_{ia}}\right)^2 + \left(\frac{U_{G_T}}{G_T}\right)^2} \quad (13)$$

where, according to Eq. (5), U_{F_R} can be calculated as the following relation with considering the negligible error in A_c

$$U_{F_R} = F_R \times \sqrt{\left(\frac{U_{\dot{m}}}{\dot{m}}\right)^2 + \left(\frac{U_{\Delta T_{ia}}}{\Delta T_{ia}}\right)^2 + \left(\frac{U_{\Delta T_{oi}}}{\Delta T_{oi}}\right)^2 + \left(\frac{U_{C_p}}{C_p}\right)^2 + \left(\frac{U_{G_T}}{G_T}\right)^2 + \left(\frac{U_{U_L}}{U_L}\right)^2} \quad (14)$$

$$U_{U_L} = U_L \times \sqrt{\left(\frac{U_{h_{rad}}}{h_{rad}}\right)^2 + \left(\frac{U_{h_{wind}}}{h_{wind}}\right)^2 + \left(\frac{U_{h_{air}}}{h_{air}}\right)^2 + \left(\frac{U_{\Delta T_{oi}}}{\Delta T_{oi}}\right)^2 + \left(\frac{U_{h_{fluid}}}{h_{fluid}}\right)^2} \quad (15)$$

Where $U_{h_{rad}}$, $U_{h_{wind}}$, $U_{h_{air}}$, $U_{h_{fluid}}$ and $U_{\Delta T_{oi}}$ are the uncertainties of h_{rad}, h_{wind}, h_{air}, h_{fluid} and ΔT_{oi} (temperature rise across the collector), respectively.

$\frac{U_{\dot{m}}}{\dot{m}} \le 0 \cdot 2\%$, $\frac{U_{h_{rad}}}{h_{rad}} \le 0.89\%$, $\frac{U_{h_{wind}}}{h_{wind}} \le 0.57\%$,

$\frac{U_{C_p}}{C_p} \le 0.1\%$, $\frac{U_{h_{air}}}{h_{air}} \le 0.125\%$, $\frac{U_{\Delta T_{oi}}}{\Delta T_{oi}} \le 0.316\%$,

$\frac{U_{h_{fluid}}}{h_{fluid}} \le 0.33\%$, $\frac{U_{U_L}}{U_L} \le 1.16\%$, $\frac{U_{\Delta T_{ia}}}{\Delta T_{ia}} \le 0.3\%$,

$\frac{U_{F_R}}{F_R} \le 2.36\%$. The maximum uncertainty obtained in the present study in determining the collector efficiency at various tests was estimated as 3.32%.

4. Results and Discussion

Experiments were conducted for several days in September between 10:00 and 16:00 h. The experimental results are presented in the form of graphs that describe the collector efficiency against the reduced temperature parameter $\frac{(T_i - T_a)}{G_T}$. All the presented data were divided into several test runs. Each test run was divided into several test periods in a quasi-steady-state condition. The maximum variations in ambient and inlet temperatures in each test period are 0.7˚C and 0.5˚C, respectively, whereas the maximum variation in the global radiation was 28 W/m^2. Hence, it was confirmed that the data presented here satisfy the necessities presented in the ASHRAE Standard 93-2003.

4.1 Water as working fluid

Figure 5 presents an example of typical recorded data for water-based fluid at 0.2 L/min (0.0033 kg/s) in one of the test days. The temperatures T_i, T_o and T_a, represent the inlet, outlet and ambient temperature of the collector. It was observed that there is a maximum temperature difference of 6°C between inlet and outlet of the solar collector at 13:30 h. The maximum incident energy on the plate of the absorber is 1108 W/m^2.

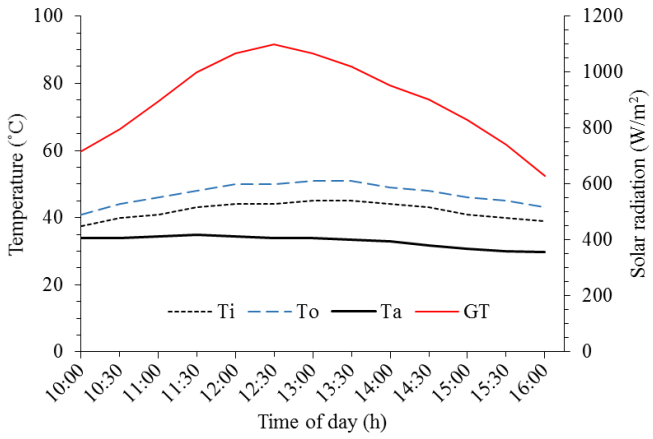

Figure 5. Transient variation in solar insolation and collector temperature.

4.2 CuO nanofluid as working fluid

Figure 6 compares the efficiency of the flat-plate collector using water and CuO nanofluid with the mass concentration of 0.2 wt.% with a fluid flow rate of 0.0033 kg/s. Values of F_RU_L and $F_R(\tau\alpha)$ are calculated and represented in Table 3. $F_R(\tau\alpha)$ is the intersection of the line with the vertical axis and nominated as absorbed energy parameter. The value of F_RU_L that is the slope of the line, nominated as the removed energy parameter. As shown in Table 3, the $F_R(\tau\alpha)$ and F_RU_L values for nanofluid were increased 5.65% and 27.87%, respectively, in comparison with water. Therefore, the increase in the maximum thermal efficiency, $F_R(\tau\alpha)$ can compensate the increase in removed energy parameter, F_RU_L. Therefore, it can be concluded that the efficiency of the solar collector was increased when using CuO nanofluids when compared with that using water.

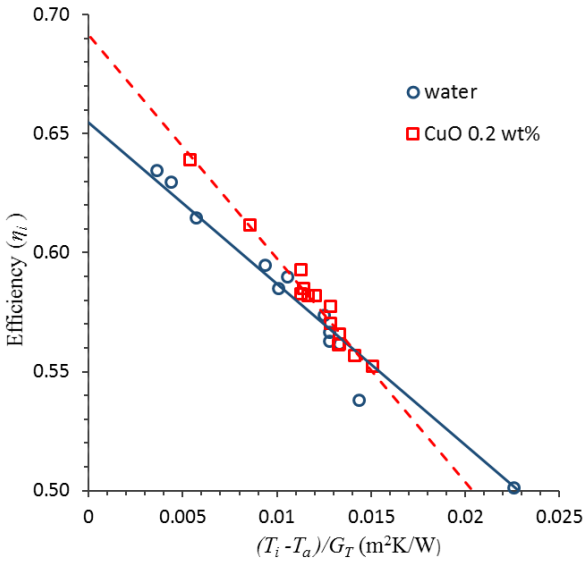

Figure 6. Flat-plate collector efficiency with water and CuO nanofluid.

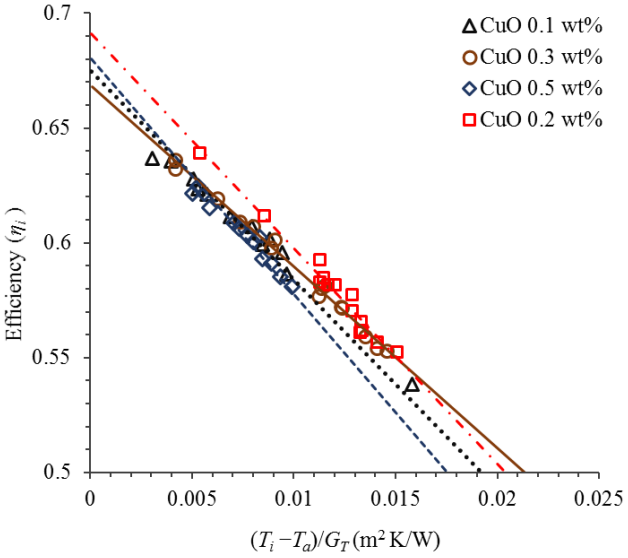

Figure 7. Effect of mass concentration of nanofluid on the flat-plate collector efficiency.

Table 3. Values of F_RU_L, $F_R(\tau\alpha)$ and R^2 for water and CuO nanofluid (0.2 wt.%).

Base fluid type	F_RU_L	$F_R(\tau\alpha)$	R^2
Water	6.7733	0.6546	0.970
CuO nanofluid (0.2 wt.%)	9.3913	0.6916	0.974

Table 4. Values of F_RU_L, $F_R(\tau\alpha)$ and R^2 for CuO nanofluid with 0.0033 kg/s mass flow rate.

CuO nanofluid (wt.%)	F_RU_L	$F_R(\tau\alpha)$	R^2
0.1	9.1096	0.6753	0.9945
0.2	9.3913	0.6916	0.974
0.3	7.9034	0.6686	0.992
0.5	10.292	0.6806	0.994

4.3 Effect of nanofluid mass concentration

The efficiency of flat-plate collector versus the reduced temperature parameter for different mass concentrations of CuO nanofluid (0.1, 0.2, 0.3 and 0.5 wt.%) is shown in Figure 7. It was observed that the efficiency of flat-plate collector for 0.2 wt.% of CuO was higher than that of all other concentrations. Ding *et al.* (2006) provided that the local heat transfer coefficient, h, can be approximately given as k/δ_t, where k and δ_t are thermal conductivity and the thickness of thermal boundary layer, respectively. Based on this idea, it may be concluded that the increasing of thermal conductivity of nanofluid compare with base fluid is smaller than the increasing of thermal boundary layer of nanofluid with respect to the base fluid. Therefore, there is a decrease in heat transfer. As can be seen from Table 4, increasing the mass concentration from 0.1 to 0.2 wt.%, the $F_R(\tau\alpha)$ and F_RU_L also increased about 2.4% and 3.1%, respectively. However, with the augmentation of nanoparticles' mass concentration from 0.2 to 0.5 wt.%, $F_R(\tau\alpha)$ decreases to 1.6% and F_RU_L increases to 9.6%, which means that according to Eq. (4), the collector efficiency decreases. The reduction in collector efficiency with increase in mass concentration beyond 0.3wt% is due to agglomeration of nanoparticles which thereby reduces the Brownian motion of the fluid and causes decrease in heat transfer.

4.4 Effect of mass flow rate

Figure 8 shows the variation in the efficiency versus reduced temperature parameter, $(T_i-T_a)/G_T$ for mass flow rates of 0.0016 and 0.0033 kg/s for nanofluid with 0.2 wt.%. $F_R(\tau\alpha)$ and F_RU_L values of the solar collector for various mass flow rates of CuO nanofluid are represented in Table 5. From Figure 8, it can be concluded that for small values of reduced temperature differences parameter, $(T_i-T_a)/G_T$, the efficiency is increased by increasing the mass flow rate. Beyond these small values, the efficiency gets a reverse trend. Therefore, due to increase of mass flow rate, the bulk temperature of CuO nanofluid is decreased. Thus, its thermal conductivity enhancement is reduced.

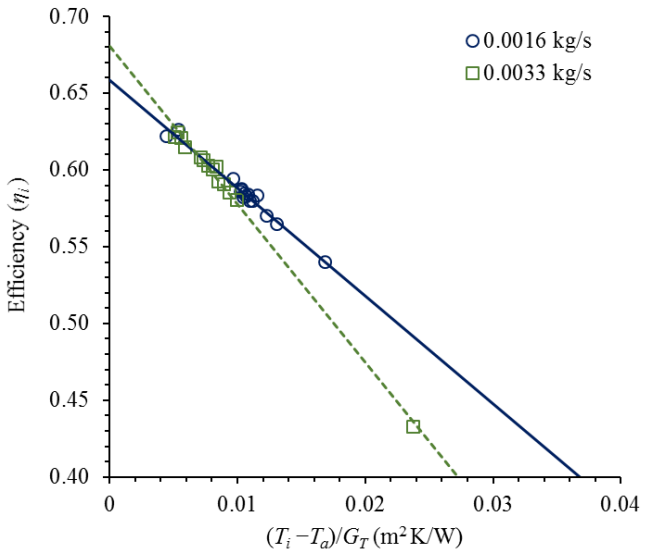

Figure 8. Effect of mass flow rate of nanofluid on the efficiency of flat-plate solar collector.

Table 5. Values of F_RU_L, $F_R(\tau\alpha)$ and R^2 for CuO nanofluid with different mass flow rate.

Mass flow rate (kg/s)	F_RU_L	$F_R(\tau\alpha)$	R^2
0.0016	7.031	0.6589	0.977
0.0033	10.292	0.6806	0.994

Figure 9 shows the strong dependence of the system efficiency on the hot fluid mass flow rate, which increases with this efficiency and with the solar radiation as presented in Figure 10. It reaches its maximum value of 64.3% for an optimal mass flow rate of 0.00695 kg/s. The fact for this increase in mass flow rate is accompanied by an increase in convection heat transfer co-efficient to the fluid, thus enhancing the rate of heat transfer to the fluid.

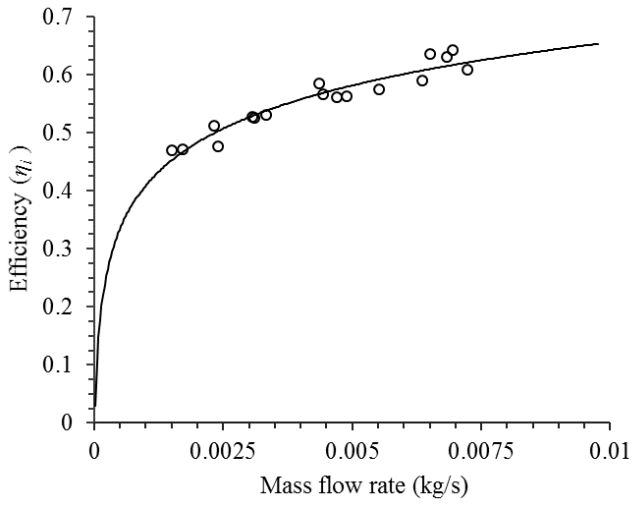

Figure 9. Collector efficiency with fluid mass flow rate.

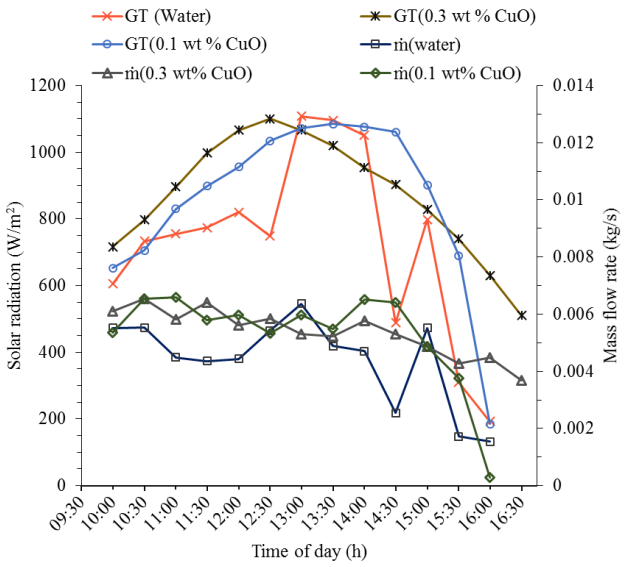

Figure 10. Solar radiation and fluid mass flow rate with time.

5. Conclusions

The effects of using CuO nanofluid as the absorbing medium on the flat-plate solar collector efficiency have been studied experimentally. The effects of mass flow rate and nanoparticles at different mass concentration are studied. The results show that higher collector efficiency was obtained for 0.2 wt.% of CuO nanofluid. From the experimental results, it was found that there was enhancement in efficiency of 5.65% for a mass flow rate of 0.0033 kg/s using CuO nanofluid. The optimum mass flow rate depends on the thermal characteristics of working fluid. For small values of reduced temperature differences parameter, the efficiency is increased by increasing the mass flow rate. Beyond these small values, the efficiency gets a reverse trend. A maximum efficiency of 64% is achieved in the present collector. Hence, it is concluded that the CuO nanofluid is one of the best fluid for enhancing the performance of thermosyphon solar water heaters.

Nomenclature

A_C	Surface area of solar collector (m^2)
C_p	Heat capacity (J/kgK)
F'	Collector efficiency factor
F_R	Heat removal factor
G_T	Global solar radiation (W/m^2)
$\dot{m}$	Mass flow rate of fluid flow (kg/s)
Q_u	Rate of useful energy gained (W)
t	Time (s)
T	Temperature (K)
U_L	Overall loss coefficient of solar collector (W/m^{2}K)
SEM	Scanning electron microscopy
HRTEM	High resolution transmission electron microscopy

Subscripts

a	ambient

bf	base fluid
i	inlet
np	nanoparticle
nf	nanofluid
o	outlet
tp	tube outlet side of the absorber

Greek symbols

$\tau\alpha$	product of absorbance and transmittance
η_i	instantaneous collector efficiency
φ	volume fraction of nanoparticles
ρ	density (kg/m^3)

Acknowledgement
The authors wish to acknowledge the Institute for Energy Studies, Anna University, Chennai, for their support rendered to carry out the research work.

References

[1] Abernethy, R.B., Benedict, R.P., Dowdell, R.B. 1983, "ASME measurement uncertainty", ASME paper 83-WA/FM-3.

[2] Ali Jabari, M., Mahmood, F.G, Mahmood, S, Monireh, H.Z., 2014, "Effects of CuO/water nanofluid on the efficiency of a flat-plate solar collector". Exp. Therm. Fluid Sci. 58, pp. 9-14.

[3] Choi, S.U.S. (1995). Enhancing thermal conductivity of fluids with nanoparticles. Tech. Rep. FED, 231.

[4] Chougule, S.S., Sahu, S.K., Ashok, T.P., 2014, "Thermal performance of two phase thermosyphon flat-plate solar collectors using nanofluid" J. Sol. Energ. Eng. 136, pp. 14503-1.

[5] Ding, Y., Alias, H., Wen, D., Williams, R.A., 2006 "Heat transfer of aqueous suspensions of carbon nanotubes (CNT nanofluids)", Int. J. Heat Mass Trans., 49, pp. 240-250.

[6] Goudarzi, K., Shojaeizadeh, E., Nejati, F., 2014 "An experimental investigation on the simultaneous effect of CuO-H_2O nanofluid and receiver helical pipe on the thermal efficiency of a cylindrical solar collector" Appl. Thermal Eng., 73, pp.1234-1241.

[7] Lee, S., Choi, S.U.S., Li, Eastman. J.A., 1999 "Measuring thermal conductivity of fluids containing oxide nanoparticles",Transaction of ASME. J. Heat Transf. 121, pp. 280-289.

[8] Lu, L., Liu, Z.H., Xiao, H.S., 2011 "Thermal performance of an open thermosyphon using nanofluids for high-temperature evacuated tubular solar collectors. Part 1: Indoor experiment" Sol. Energy 85, pp. 379-387.

[9] Nada, S.A., El-Ghetany, Hussein, H.M.S.,2004 "Performance of a two-phase closed thermosyphon solar collector with a shell and tube heat exchanger" Appl. Therm. Eng. 24, pp. 1959-1968.

[10] Norton, M.S., 2010. Uncertainty Analysis.

[11] Otanicar, T.P., Phelan, P.E., Prasher, R.S., Rosengarten, G., Taylor, R.A.,2010 "Nanofluid based direct absorption solar collector" J. Renew. Sustain. Energy 2, pp.33-102.

[12] Shojaeizadeh, E., Veysi, F., Yousefi, T., Davodi, F., 2014 "An experimental investigation on the efficiency of a flat-plate solar collector with binary working fluid: A case study of propylene glycol (PG)-water" Exp. Therm. Fluid Sci. 53, pp. 218-226.

[13] Wang, X., Xu, Choi, S.U.S., 1999 "Thermal conductivity of nanoparticle fluid mixture" J. Thermophys. Heat Trans. 13, pp. 474-480.

[14] Wei, L.J., Yuan, D., Tang, D., Wu, B., 2013 "A study on a flat-plate type of solar heat collector with an integrated heat pipe" Sol. Energy 97, pp.19-25.

[15] Yousefi, T., Veysi, F., Shojaeizadeh, E., Zinadini, S., 2012 "An experimental investigation the effect of Al_2O_3-H_2O nanofluid on the efficiency of flat-plate solar collectors" Renew. Energ. 39, pp. 293-298.

[16] Yousefi, T., Veysi, F., Shojaeizadeh, E., Zinadini, S, 2012 "An experimental investigation on the effect of MWCNT-H_2O nanofluid on the efficiency of flat-plate solar collector" Exp. Therm. Fluid Sci., 39, pp. 207-212.

[17] Yousefi, T., Veysi, F., Shojaeizadeh, E., Zinadini, S., 2012 "An experimental investigation on the effect of pH variation of MWCNT-H_2O nanofluid on the efficiency of a flat-plate solar collector" Sol. Energy 86, pp. 771-779.

[18] Zerrouki, A., Boumedien, A., Bouhadef, K., 2002 "The natural circulation solar water heater model with linear temperature distribution" Renew. Energ., 26, pp. 549-559.